Bulgarian Chemical Communications, Volume 51, Special Issue D (pp. 77 – 84) 2019

General characteristics of silver nanoparticles analysis by single particle inductively coupled plasma mass spectrometry

V. M. Stefanova*, L. I. Kaynarova, D. L. Georgieva

University of Plovdiv "Paisii Hilendarski";Department of Analytical Chemistry and Computer Chemistry, 24 Tzar Assen Str.,4000 Plovdiv, Bulgaria

Received December 10, 2018; Revised January 18, 2019

Single particle inductively coupled plasma mass spectrometry (spICP-MS) is a new powerful and sensitive technique for detecting, characterizing, and quantifying nanoparticles in suspension. The possibility to detect in a single run the presence of both dissolved and particulate forms of an element is promising in the context of nanotoxicology studies. In order to obtain adequate information, the recorded peak must be produced by a single nanoparticle, which automatically leads to several challenges – appropriate dilution providing separation of the signals generated from the individual particles, stabilization of the introduced nanocolloidal suspension, and recording of fast peak signals.

In the current study a model for theoretical calculation of the dilution factor of AgNPs with different size is applied ensuring optimal peak frequency. Various reagents and washing solutions such as non-ionic surfactants (TX-100, TX-114), buffers and acid solutions were tested for stabilization of the sample introduction of Ag nanocolloidal suspension, aiming to decrease transport losses and "memory effect". Some general characteristics of AgNPs analysis by spICP-MS as: particle number concentration (#Particles L^{-1}), separate evaluation of mass concentration of NPs and ionic silver and corresponding % fraction of nanoparticles in suspension were estimated. The method was applied for analysis of three nanocolloidal suspensions - one synthesized in our lab and two commercial products.

Keywords: Silver nanoparticles; Single particles; Inductively coupled plasma mass spectrometry; Characterization

INTRODUCTION

The rapid development of nanoscience and nanotechnology in the last decade leads to intensive use of nanosized materials in different fields of human life. According to the statistics of the Emerging nanotechnologies program, up to 2014 there are more than 1800 products with engineered nanomaterials, released on the markets in 32 countries, and more than 440 (24%) of them contain silver nanoparticles (AgNPs) [1, 2]. Due to their unique properties they find application in drug delivery, cosmetics, water purification systems and other products [2, 3]. The everyday use of products which contain silver nanoparticles leads to their release in the environmental system. A good understanding of their ecological cycle and assessment of human health risk requires not only detection and quantification but also physicochemical characterization as shape, size, diameter, surface charge [4].

Different types of techniques such as: i) electron microscopy - transmission electron microscopy (TEM) and scanning electron microscopy (SEM); ii) optical spectroscopy - UV-visible spectroscopy (UV-vis), dynamic light scattering (DLS); iii) atomic spectroscopy methods and electrochemical methods are exploited for characterization of AgNPs [5, 6]. A powerful technique for nanoparticles characterization, evolved recently, is the single particle inductively coupled plasma mass spectrometry (spICP-MS) which combines the low limits of detection (ng L^{-1}) and the high sensitivity of ICP-MS with a new single particle detection mode [7–10]. The theoretical principle of this method was developed by Degueldre *et al*. [11] who demonstrated the capability of ICP-MS for single particle analysis of colloids in water. According to the theory of the method it is expected that each particle produces in the plasma a flash of ions originating a fast transient signal that can be measured. The fundamental prerequisites for registration of single particle events are: sufficiently large dilution that provides separation of the peaks generated by individual nanoparticles and fast detection system working with short dwell times (10 ms or less). If the number of particles in suspension is low enough, then only one particle will reach the plasma at a time, producing a spike with intensity above the background which represents the ionic concentration of "dissolved" material in solution. Thus, the frequency of the pulse is directly related to the number concentration of particles. Degueldre *et al.* relate the frequency of the particle events (N_p), to the particle number concentration (C_{NPs}, #Particles L^{-1}). For suspensions of nanoparticles measured by the spICP-MS method, C_{NPs} can be

* To whom all correspondence should be sent.
E-mail: stefanova@uni-plovdiv.net

expressed as:

$$C_{NPs} = Np \times \frac{1}{\eta_n} \times \frac{1}{V} \times \frac{1}{T} \times 10^3, \quad (1)$$

where: Np – nanoparticle events measured; η_n- transport efficiency; V - sample uptake flow rate, (ml min^{-1}); T – total acquisition time, (min).

The transport efficiency can be calculated in several ways [12]: i) as the ratio of sample uptake and drain flow rates; ii) by the certified diameter of a reference material; iii) by the mass concentration of a reference material. Correct determination of η_n is necessary for calculation of particle number concentration.

The intensities of registered peaks are proportional to the mass of NPs and are therefore related to their size. So the smallest detectable size of nanoparticles is element specific and will depend on both instrument sensitivity and background level. An approximate estimation of the background signal contribution can be made by calculating the Background Equivalent Diameter (BED) which represents the average continuous signal (originating from ionic concentration), over which the peaks should be statistically distinguished. The BED is an estimate analogous to the Background Equivalent Concentration (BEC) used in the optical spectral methods.

As the spICP-MS method is capable of measuring nanoparticles mass concentration together with the ionic concentration of the carrier solution, the mass distribution between both phases (NPs and ionic) can also be evaluated.

Despite the growing number of recent publications devoted to AgNPs characterization by spICP-MS some general issues are still under investigation such as: stabilization of working solutions containing NPs; memory effect and protocols of washing; validation of methods for estimation of particle number concentration and distribution of Ag between solid and liquid phases of a nanocolloidal system. Last but not least, controlling the dilution of nanocolloids is crucial to ensure both the registration of single particle events together with the accumulation of a sufficiently large data set for subsequent statistical processing that allows a reliable interpretation of the results. The aim of this work was to characterize suspensions of silver nanoparticles with different size (RM AgNPs 60 nm, RM AgNPs 40 nm and AgNPs synthesized by us with unknown size). For this purpose, we proposed a model for theoretical calculation of the dilution factor of silver nanoparticles ensuring an optimal peak frequency. The model allows predicting the number of nanoparticles expected to be recorded, depending on the input data for the size and mass concentration of the samples, together with instrumental parameters of the measurement itself.

EXPERIMENTAL

Instrumentation and reagents

ICP-MS 7700 Agilent spectrometer with MicroMist™ nebulizer and Peltier cooled double pass spray chamber was used for silver nanoparticles determination at a mass of 107 amu. The ICP-MS operating parameters are as follow: RF power - 1.55 kW; sample flow rate - 0.342 mL min^{-1}; carrier Ar gas flow rate - 1.1 L min^{-1}. Data were collected at time resolved analysis (TRA) acquisition mode with 5 ms integration time for 60 s acquisition time.

UV-vis spectra were recorded using a ONDA spectrophotometer UV-30 SCAN in absorbance mode within the wavelength range 200 – 600 nm with a scanning step of 2 nm.

For sonication of silver colloids an ultrasonic bath (Kerry US) was used.

Certified reference materials of AgNPs suspensions with two different sizes (40 nm ± 4 nm, and 60 nm ± 8 nm) and mass concentration 0.02 mg mL^{-1} were purchased from Sigma-Aldrich. Two commercial products "Silver water" with declared presence of Ag NPs and mass concentration of silver 10 mg L^{-1} were purchased from local pharmacies.

$AgNO_3$ (Merck, p.a), H_2O_2 (30%, Valerus, p.a.), $NaBH_4$ (Acros Organics- Fisher-Scientific, 98+%) and sodium citrate tribasic monohydrate – TSC (Chemsnab Dimitrovgrad, p.a.) were used for synthesis of silver nanoparticles. Single standard solution of Ag 1000 mg L^{-1} was purchased from Merck. Nitric acid HNO_3 (65% Fluka p.a.), nonionic surfactants TX–114 (Fluka AG, p.a.), TX–100 (Fisher-Scientific, p.a.) and citrate buffer (0.1 mol L^{-1}) prepared in our lab were tested as washing and stabilization agents. All suspensions and solutions were prepared by dilution with double distilled water (BDW).

The raw data obtained from spICP-MS measurements were statistically evaluated by MassHunter Workstation Single Nanoparticle Application (Rev. A, June 2017; Agilent Technologies) and Excel (Microsoft).

Sample preparation

Synthesis of silver nanoparticles. Methodology for synthesis of AgNPs was taken from [13]. Briefly, 50 µl of $AgNO_3$ (0.05 mol L^{-1}), 0.5 ml of TSC (75 mmol L^{-1}), 60 µl of 30% H_2O_2, and 250 µl of $NaBH_4$ (100 mmol L^{-1}) were added

into 24.14 ml of BDW at room temperature under vigorous stirring for 30 min.

Sample preparation for quantitative analysis. All dilute samples, as well as intermediate standards were daily prepared. Based on our theoretical model, samples for spICP-MS analysis were prepared with different dilution factors (DF) as follows: i) RM AgNPs 60 nm, DFs 8×10^4 and 1.6×10^5; RM AgNPs 40 nm, DFs in the interval $2.7\times10^5 \div 1\times10^6$; iii) Ag NPs synthesized in the lab, DF 1×10^5; and iv) commercial products, DF 5×10^4. These factors were achieved with two-step dilution. All samples and RMs were treated in an ultrasonic bath for 30 min before and after dilution to guarantee homogeneous distribution of AgNPs in solution. Ionic standard solution of Ag (1 μg L^{-1}) was used to assess instrument signal response for silver and as calibrator for mass concentration determination. RM AgNPs 40 nm was used as a reference material for calibration by size. The other materials were measured only as samples. Transport efficiency was evaluated by the size of reference material. In order to decrease transport losses and memory effect, a comparison of a variety of washing and stabilization reagents was made: 5% solution of HNO_3, 0.1 mol L^{-1} citrate buffer, 0.5% solutions of non-ionic surfactants (TX–114 and TX–100).

For UV-vis detection all samples were diluted by a DF=10.

RESULTS AND DISCUSSION

Theoretical calculation model for dilution of NPs prior to spICP-MS measurement

Appropriate dilution of the nanoparticulate suspension is a key parameter which affects both the possibility of separate registration of the individual particle events and the accumulation of sufficient data for adequate statistical processing of the measured signals. The basic assumption of spICP-MS that each recorded signal represents a single NP motivated us to develop a model for theoretical calculation of the dilution factor of AgNPs, to guarantee optimal peak frequency (table 1).

This model represents the quantitative relation between size, mass and number of atoms of one nanoparticle (Eq. 2) which allows us to calculate the expected number of nanoparticles (NP) in 1 ml of solution with a given mass concentration (assigned to NPs content) (Eq. 3):

$$No_{atoms}/NP = \frac{\frac{1}{6}\times\pi\times d^3\times\rho\times f\times 6.02214\times10^2}{A_m} \quad (2)$$

$$\#Particles/ml = \frac{C_{sample}\times6.02214\times10^7}{A_m\times No_{atoms}/NP} \quad (3)$$

where: d is diameter of NPs in nm; ρ is NPs material density in g cm^3; f is mass fraction of analyte; A_m is atomic mass of analyte in g mol^{-1}; C_{sample} is mass concentration of NPs in suspension in mg L^{-1}

The model incorporates the current instrumental parameters influencing both sample transport through the nebulization system (i.e. sample flow rate and nebulization efficiency) and timing. Time parameters of the measurement - single measurement time (integration time - t_d) and whole time for data collection (acquisition time – t_{acq}) determine the total number of measurements to be recorded for the sample.

To ensure effective separation of the signals generated by nanoparticles from the baseline produced by dissolved analyte in the carrier solution, we set the condition to have a ratio of approximately 1:10. The latter provides an optimal frequency of nanoparticle events together with accurate measurement of the baseline.

Hence, the desired number of particles corresponding to the commented above condition could be defined before analysis. In the case of the current study, with time parameters given in table 1, 12000 data points were measured per single replicate. Thus, 1200 is the number of desired nanoparticles in sample solution. The dilution factor was calculated as a ratio of expected and desired number of peaks (Eq. 4):

$$DF = \frac{No\ peaks_{exp}}{No\ peaks_{des}} = \frac{\#Particles/ml\times\eta_t\times V\times t_d}{t_{acq}\times10^2} \quad (4)$$

where: η_t is transport efficiency; V is sample flow rate in ml min^{-1}; t_d is integration time in ms; t_{acq} is acquisition time in sec.

The theoretical model includes preliminary data, such as the diameter and mass concentration of nanoparticles, which are commonly available for certified reference materials or engineered NPs. For unknown samples the application of the described model requires some preliminary measurements. The tentative size of silver nanoparticles could be obtained from the UV-vis spectrum, while mass concentration could be determined by spectrochemical analysis of digested sample.

Table 1. An example for application of the calculation model for NPs suspension dilution of RM AgNPs 40 nm before spICP-MS determination

NPs Characteristics			
Analyte	Ag	Density (g cm^{-3})	10.49
Atomic mass - A_m(g mol^{-1})	107.8682	Analyte mass fraction	1
Preliminary data		Calculations	
Diameter - d (nm)	40	No of atoms/NPs	1.96×10^{6}
Conc sample (mg L^{-1})	20	NPs conc (# Particles mL^{-1})	5.69×10^{10}
SP-ICP-MS parameters		Expected No of peaks	1.28×10^{9}
Sample flow rate – V (mL min^{-1})	0.342	No of data points for acquisition	12000
Transport efficiency	0.066		
Integration Time (ms)	5	Desired No of peaks	1200
Acquisition Time (s)	60	Dilution Factor	1.07×10^{6}

UV-vis spectral characterization of AgNPs

As is well known, Ag colloids show a strong plasmon resonance band in which the maximum wavelength depends on particle size and shape [14, 15]. In the current work this specific behavior was used to obtain preliminary information about the mean size of a sample of AgNPs synthesized by us according to the procedure described by Yan *et al.* [13] and for comparison the two RM AgNPs, 60 nm and 40 nm were measured as well. The registered UV-spectra are presented on fig. 1.

The wavelengths of the maxima of plasmon resonance peaks for AgNPs in the tested RMs are in agreement with the spectral data provided by the manufacturer (i.e. λ_{max} in the range of 405-425 nm and 425-450 nm for AgNPs with diameter 40 and 60 nm, respectively) with well distinguished "blue" shift typical for NPs with smaller size [14]. The lowest wavelength of the maximum (λ_{max}=390 nm), recorded for the AgNPs synthesized by us, corresponds to a mean diameter of ~ 20 nm [16]. The clear shift of the peak maxima over the diameter of the silver nanoparticles allows a rapid preliminary estimation of the particle size in an unknown sample and thus a correct dilution of the sample for spICP-MS measurement could be calculated.

In addition, the UV-spectra of AgNPs can be used for evaluation of the stability of nanocolloidal systems.

Using the above described information the following DFs were calculated for NPs measured in the current study: 3.2×10^{5} for RM AgNPs 60 nm; 1.1×10^{6} for RM AgNPs 40 nm; 2.1×10^{5} for AgNPs synthesized in the lab (d ~ 20 nm; mass concentration - 5 mg L^{-1}); 1.3×10^{6} for the commercial products.

Study of memory effect and stabilization of AgNPs

In the numerous articles published in the scientific journals on spICP-MS no comments were found regarding the memory effect during the introduction of highly diluted nanocolloidal systems. However, some authors draw attention to the need for a relatively long stabilization time prior to measuring the sample. Our experiments showed a strong memory effect, i.e., when measuring a blank immediately after the sample many peaks originated by NPs remaining along the transport path were observed. Thus a variety of washing solvents were tested - nitric acid; citrate buffer and two surfactants, TX-100 and TX-114. For evaluation of the washing ability of the tested solvents, the measurement was performed after introduction of a sample containing Ag NPs and 2 min washing. The total signals acquired (counts for Ag) for washing solvents were compared to that obtained for a blank sample (St0) measured before introduction of NPs. The best washing properties shows nitric acid, where the overall Ag signal was ~ 30% higher than in the blank sample and only 5 NPs peaks were identified. For the other tested washing solutions (citrate buffer, TX-100 and TX-114) the signals exceeded the background by factors of 9, 11 and 14, respectively, and the number of identified peaks increased in the same order (150, 170 and 440). The ability of HNO_3 to dissolve AgNPs left on the capillary walls is probably the reason of the best washing effect. Therefore, it was used in all subsequent studies.

The carrier solvent composition affects two factors, on the one hand it stabilizes the nanocolloidal system and, on the other hand, it determines the equilibrium between solid and liquid phases (i.e., AgNPs/Ag^{+}). The first effect is important for the precision of NPs concentration

determination, while the second one is crucial for the baseline Ag^+ signal over which the peaks of NPs appeared and determined the corresponding Background Equivalent Diameter (BED) of a running measurement. Four carrier solutions of diluted AgNPs were tested: pure water (BDW); citrate buffer and non-ionic surfactants, TX-100 and TX-114.

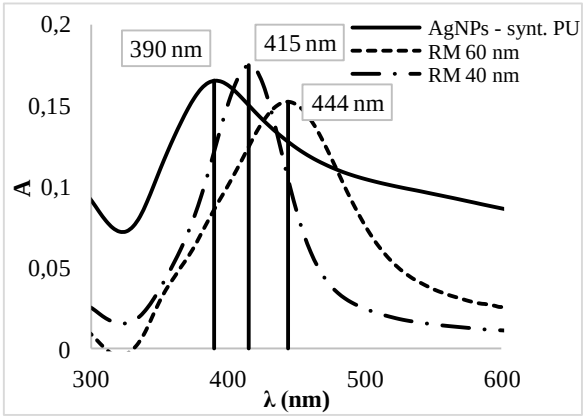

Fig. 1. UV-vis spectra of nanocolloidal suspensions from two RMs of AgNPs 60nm and 40nm and AgNPs synthesized in our lab.

As can be seen from the stability tests (figure 2), non-ionic surfactants are not suitable carriers for AgNPs for two reasons: the number of registered peaks is by about 25% lower than the corresponding one in pure water or citrate buffer; in addition, a gradual decrease of peak numbers in successively measured replicas was observed. The commented effect may be due to modification of the walls of the sample introduction tubing with a surfactant that can capture AgNPs and thereby increase transport losses. The latter is in agreement with our previous studies demonstrating that surfactants are not effective as washing solvents.

Concerning the second effect – the concentration of ionic silver that determines the baseline signal and could be assessed by BED, the obtained values were as follows: 18 nm for citrate buffer; 13 nm for BDW and 10 nm for TX-100 and TX-114. Probably, both surfactants are able to prevent silver nanoparticles from dissolving by creating a micellar environment, thus resulting in minimal silver ion signals which are preferable in determination of particles with a smaller size. But in this case the problem with transport losses still has to be overcome. The best compromise between maximum particle counting capabilities while maintaining a minimum level of background signal is the use of BDW as a carrier solvent. Under the established protocol the RM AgNPs 40 nm diluted by BDW was measured 3 consecutive times with intermediate washing by 5% HNO_3. The relative standard deviation (RSD%) of the number of NPs measured was 7.5%. In order to check the stability of the peaks appearance within the time of a single measurement, the total acquisition time (60 s) was divided into three segments (0-20 s; 20-40 s and 40-60 s) and the relative standard deviation within the mentioned segments was compared.

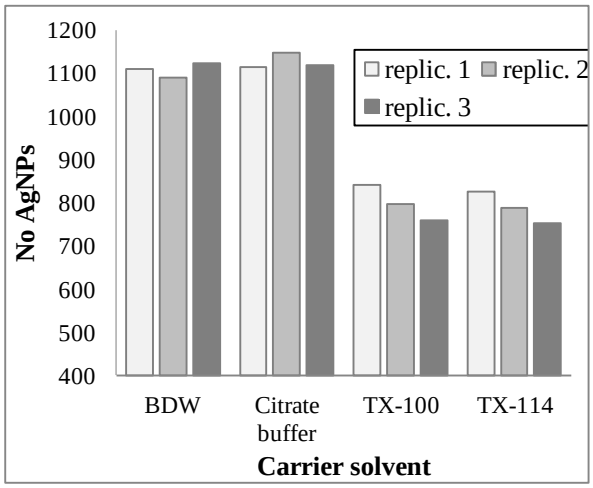

Fig. 2. Effect of the carrier solvent on the number of registered particles in three consecutive replicates upon introduction of RM AgNPs 60nm at a concentration of 125 ng L^{-1}

The results showed that the reproducibility of peaks appearance within the time segments of a single acquisition cycle is much better (RSD in the range of 2.5-4.9%) than that between parallel measurements. An attempt was made to improve the NPs counting repeatability by removing the washing step between parallel replicates. As a result, for 3 consecutive measurements of diluted RM 60 nm with a mass concentration of 250 ng L^{-1} the RSD (of number of peaks counted) was reduced down to 2.6%. Therefore, it is recommended that the washing cycle (to remove the memory effect by 5% HNO_3) be performed only between different samples, then the next measurements to be carried out on prolonged (up to 2-3 min) stabilization time without intermediate washing.

Estimation of nanoparticles mass fraction in dilute Ag NPs suspensions

One of the undisputed advantages of spICP-MS methodology is the possibility of simultaneous observation of signals generated by nanoparticles and ions in the carrier solution, on the basis of which it is possible to assess the distribution of nanoparticulate components between the two phases of the colloid system. The special software package for single particle mode of operation of ICP-MS instruments offers an option together with statistical evaluation of NPs peaks the ionic

concentration of target element to be reported by single point calibration using an ionic standard (usually at a concentration of 1 μg L^{-1}). As discussed above, good separation of peaks from single nanoparticles is achieved at very low mass concentrations of the colloids (ng L^{-1}). Unfortunately, because of the huge dilution factors in combination with the very short measurement time, in most of the optimization studies it was impossible to estimate the concentration of silver ions. Therefore, we propose a new approach to assessing the distribution of silver between solid and liquid phases from a single measurement. The percent mass fraction of AgNPs was evaluated by the ratio of the summarized signals for all registered NPs peaks to the total signal measured for the specific replicate. It should be noted that blank subtraction is applied before calculation. The results obtained for both tested RMs of citrate stabilized AgNPs are presented in Table 2.

The possibility to estimate the mass fraction of NPs in reference materials for particles characterization is an important issue, because most of the manufacturers include in the certificate the total mass concentration of the material together with the data about mean diameter with corresponding size uncertainty. This hampers the validation of analytical procedures for determination of particle number concentration.

Table 2. Percent mass fraction of Ag incorporated in NPs in two reference materials (Sigma Aldrich) with different particle diameters

Type of RM	AgNPs 40 nm (75 μg L^{-1})			AgNPs 60 nm (250 μg.L^{-1})		
Replicate No	1	2	3	1	2	3
Sum of NPs peaks (counts)*	91050	96938	103709	274489	265295	256551
Sum of all signals (counts)*	104621	112292	121818	377564	367024	364639
% mass fraction of AgNPs	87.0	86.3	85.1	72.7	72.3	70.4
	Average	SD	RSD %	Average	SD	RSD %
% AgNPs	86.2	1.0	1.1	71.8	1.2	1.7

*The corresponding blank signals are previously subtracted

Table 3. Detected number of particles in two reference materials with different diameters and dilution factors

Type of RM	Total mass concentration RM (ng L^{-1})	Corrected mass concentration (ng L^{-1})*	Detected number of particles		Calculated number of particles**	Recovery %
			Average number (n=3)	RSD %		
Ag NPs 40 nm	50	43	2437	0.7	2762	88
	20	17	1053	2.1	1106	95
Ag NPs 60 nm	250	180	2175	2.6	2597	84
	125	90	1209	2.7	1295	93

* The total mass concentration of RM was corrected taking into account the corresponding mass fractions of AgNPs listed in table 2. ** The specified number of nanoparticles was calculated by the proposed above theoretical model taking into account the transport efficiency of the current measurement.

Determination of Ag nanoparticle number concentration

Under the optimized measurement protocols discussed above the diluted solutions of two RMs for AgNPs with certified size and total mass concentration were subjected to spICP-MS analysis and the data are presented in table 3.

For each test material, two samples with different DFs were measured. The average values of the number of NPs of 3 consecutive measurements, as well as the relative standard deviation in %, are presented. It is clear that the number of identified nanoparticles decreases in proportion to the mass concentration of silver in the diluted solutions for both RMs.

In order to validate the applicability of the developed spICP-MS method for correct determination of particle number concentration, the experimental results were compared to the calculated ones obtained by the theoretical model. In this calculation the total mass concentration of Ag in the samples was corrected by the % fraction of AgNPs, determined experimentally (see Table 2) also including the transport efficiency of the current measurement. The presented evaluation demonstrates that recoveries > 84% are obtained in all cases. It is noted that for both materials the

recovery decreases as the number of recorded peaks increases, which can be caused by simultaneous reading of the signals from two NPs. In the investigated range of particle concentrations, this effect is not very pronounced, but confirms our hypothesis that the dilution factor for an individual nanocolloid is essential to the accuracy of the data obtained through the spICP-MS methodology.

The developed spICP-MS method was applied for determination of particle number concentration in AgNPs suspension synthesized in our lab and in two commercial products containing silver nanoparticles according to the manufacturer's declaration ("Silver water"). The RM AgNPs 40 nm was used for estimation of transport efficiency and as a standard for nanoparticles size determination. The instrument response factor and calibration for mass concentration were calculated by measurement of an ionic standard of Ag (1 μg L^{-1}). The obtained results for particle number concentration, mass concentration of nanoparticles and Ag ions in samples with corresponding percent mass fraction of silver NPs are summarized in table 4. In both commercial products, the presence of silver nanoparticles with mean size around 30 nm and concentration in the range of $10^8 – 10^9$ NPs per mL was proven. The percent fraction of AgNPs was determined in two of the analysed samples – AgNPs synthesized in our lab and "Silver water" #1. To ensure an optimal peak frequency in the samples containing a low percentage of nanoparticle fraction (5% and 40.2% for the commercial product and for the NPs synthesized in our lab), the dilution factor was reduced in comparison to the one predicted by the theoretical model (the applied dilutions are noted in table 4).

The data from the analysis show significant differences between the tested two commercial products "Silver Water", both in terms of concentration of AgNPs and of the content of silver ions. This indicates that the developed spICP-MS method is suitable for assessing both the total silver content and silver nanoparticles in commercially available products.

The size distribution diagrams for the two tested RM AgNPs (40 nm and 60 nm) and for Silver water #1 are presented on figure 3. The estimated mean sizes, as well as the corresponding size distribution for both reference materials are consistent with the certified values (i.e, 40 nm ± 4 nm, and 60nm ± 8 nm) which prove the reliability of the spICP-MS for characterization of silver nanoparticles. The mean size of NPs in Silver water #1 was determined to 30 nm with asymmetric size distribution (fig. 3C), while high concentration of ionic silver leads to increasing of steady-state signal shown on the time-resolved graph (fig. 3D) and corresponding rise of the BED diameter (see table 4).

CONCLUSIONS

The proposed model for calculating the dilution factor of samples containing silver nanoparticles allows reliable control of the desired detection rate of single nanoparticles for materials of known diameter and mass concentration. The preliminary information on size and total mass concentration of real samples subjected to the characterization of silver nanoparticles can be provided by successful combination of two spectral methods - UV-vis spectra and preliminary ICP-MS analysis. Optimized protocols for washing and stabilization of nanoparticles in the carrier solutions allow an adequate determination of AgNps concentration with recoveries between 84 and 95%. The developed spICP-MS method is capable of estimating AgNPs concentration, as well as the distribution of silver between solid and liquid phases in real samples.

***Acknowledgements**: The current work has been developed as a part of project DN19/9 2018 – 2020 (INISA) financed from the National Science Fund of Bulgaria. D. Georgieva is thankful to the National Program of Ministry of education and science "Young Scientists and Postdoctoral Students" (PMC 577/2018) for financial support.*

Table 4. Results from spICP-MS analysis of two commercial products and AgNPs synthesized in our lab.

Sample Name	# of Particles	Particle Conc. (#particles mL^{-1})	Mass Conc. (mg L^{-1})	Ionic Conc. (mg L^{-1})	BED (nm)	Mean Size (nm)	AgNPs (%)
*Silver Water #1	867 ± 49	$2.10^9 \pm 1.10^8$	0.40 ± 0.02	7.6 ± 0.7	36.5 ±0.9	30.4± 0.3	5.0 ± 0.2
*Silver Water #2	153 ± 14	$3.10^8 \pm 3.10^7$	0.12 ±0.02	< 0.1	10.7 ±0.4	29±2	-
**AgNPs PU	730 ± 28	$3.10^9 \pm 1.10^8$	1.8 ±0.2	2.8 ± 0.3	10.9± 0.4	23±1	40.2 ±1.6

*DFs for „Silver water" samples were 5×10^4. **DF for AgNPs PU was 1×10^5

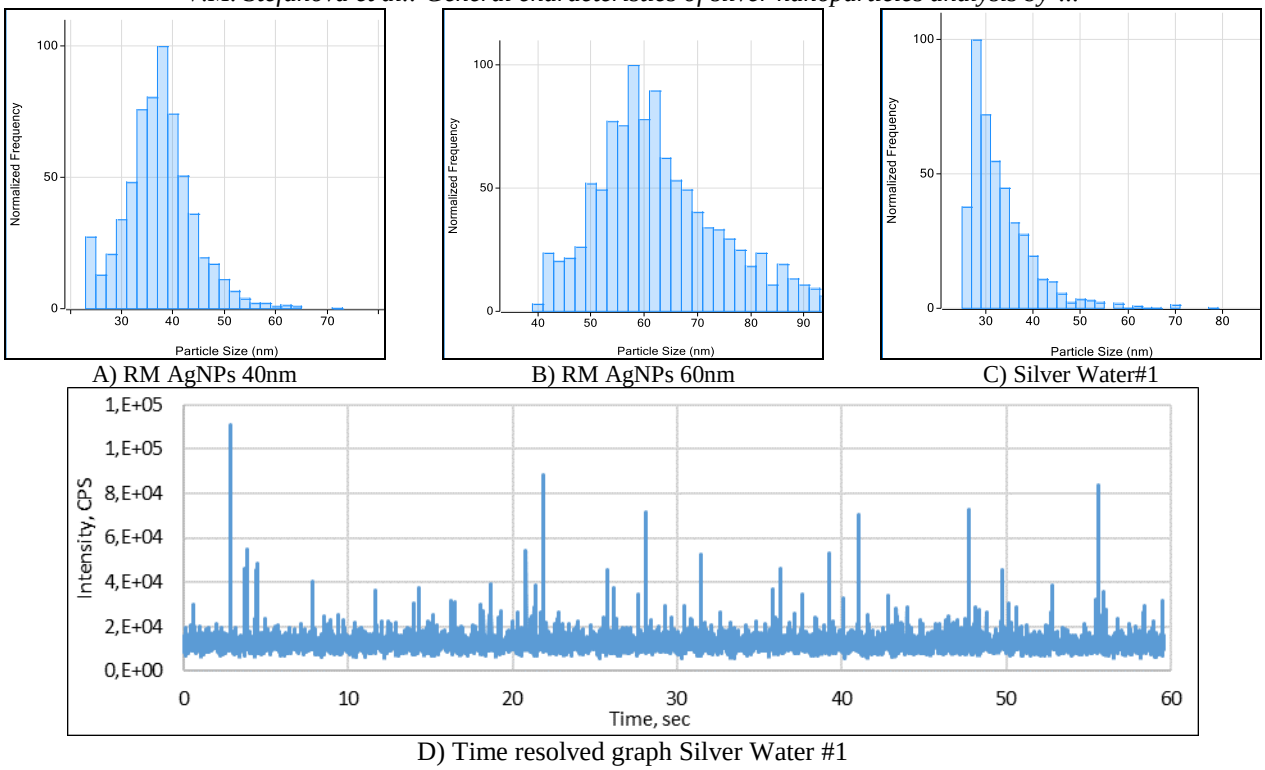

A) RM AgNPs 40nm B) RM AgNPs 60nm C) Silver Water#1

D) Time resolved graph Silver Water #1

Fig. 3. Size distribution diagram of A) RM AgNPs 40 nm; B) RM AgNPs 60 nm; C) Silver water#1 and D) time-resolved data record for Silver water #1

REFERENCES

1 Consumer Products Inventory, [Online], Available: http://www.nanotechproject.org/cpi/. [Accessed: 13-Nov-2018].

2 M. E. Vance, T. Kuiken, E.P. Vejerano, S.P. McGinnis, M.F. Hochella Jr., D. Rejeski, M.S. Hill, *Beilstein J. Nanotechnology*, **6**, 1769, (2015).

3 A. Kaphle, P. N. Navya, A. Umapathi, H. K. Daima, *Environ. Chem. Lett.*, **1**, (2017).

4 M. Bundschuh, J. Filser, S. Lüderwald, M.S. McKee, G. Metreveli, G.E. Schaumann, R. Schulz, S. Wagner , Nanoparticles in the environment: where do we come from, where do we go to?, *Environmental Sciences Europe*, **30**, 1. (2018).

5 F. Laborda, E. Bolea, G, Cepriá, M.T. Gómez, M.S. Jiménez, J. Pérez-Arantegui, J.R. Castillo, *Anal. Chim. Acta*, **904**, 10, (2016).

6 S. Palchoudhury, M. Baalousha, J. R. Lead, Characterization of nanomaterials in complex environmental and biological media, 8. Elsevier, 2015.

7 F. Laborda, E. Bolea, J. Jimenez-Lamana, J. Jiménez-Lamana, *Anal. Chem.*, **86**, 2270, (2014).

8 M. D. Montaño, J. W. Olesik, A. G. Barber, K. Challis, J. F. Ranville, *Anal. Bioanal. Chem.*, **408**, 5053 (2016).

9 F. Laborda, E. Bolea, J. Jiménez-Lamana, *Trends Environ. Anal. Chem.*, **9**, 15 (2016).

10 K. E. Murphy, J. Liu, A. R. M. Bustos, M. E. Johnson, M. R. Winchester, *NIST Spec. Publ. 1200-21*, (2015).

11 C. Degueldre P. Y. Favarger, *Colloids Surfaces A Physicochem. Eng. Asp.*, **217**, 137 (2003).

12 H. E. Pace, N. J. Rogers, C. Jarolimek, V. A. Coleman, C. P. Higgins, J. F. Ranville, *Anal. Chem.*, **83**, 9361 (2011).

13 Y. Yan, K. Bin Chen, H. R. Li, W. Hong, X. Bin Hu, Z. Xu, *Trans. Nonferrous Met. Soc. China (English Edn.)*, **24**, 3732 (2014).

14 E. Saion, E. Gharibshahi, K. Naghavi, E. Saion, E. Gharibshahi, K. Naghavi, *Int. J. Mol. Sci.*, **14**, 7880 (2013).

15 J. Krajczewski, K. Kołataj, A. Kudelski, *RSC Adv.*, 7, 17559, (2017).

16 SIGMA ALDRICH Product specification N 730793. [Online], Available: https://www.sigmaaldrich.com/Graphics/COfAInfo/SigmaSAPQM/SPEC/73/730793/730793-BULK_ALDRICH_pdf. [Accessed: 13-Nov-2018].